

The Mre11 Complex Is Required for Repair of Hairpin-Capped Double-Strand Breaks and Prevention of Chromosome Rearrangements

Kirill S. Lobachev, Dmitry A. Gordenin,
and Michael A. Resnick¹

Laboratory of Molecular Genetics
National Institute of Environmental Health Sciences
National Institutes of Health
Research Triangle Park, North Carolina 27709

Summary

Inverted repeats (IRs) that can form a hairpin or cruciform structure are common in the human genome and may be sources of instability. An IR involving the human *Alu* sequence (*Alu*-IR) has been studied as a model of such structures in yeast. We found that an *Alu*-IR is a mitotic recombination hotspot requiring *MRE11/RAD50/XRS2* and *SAE2*. Using a newly developed approach for mapping rare double-strand breaks (DSBs), we established that induction of recombination results from breaks that are terminated by hairpins. Failure of the *mre11*, *rad50*, *xrs2*, and *sae2* mutants to process the hairpins blocks recombinational repair of the DSBs and leads to generation of chromosome inverted duplications. Our results suggest an additional role for the Mre11 complex in maintaining genome stability.

Introduction

Gross chromosome rearrangements are often found in tumor (Schar, 2001) and drug-resistant cells (Windle and Wahl, 1992) and are associated with many inherited diseases (Timme and Moses, 1988). Large inverted duplications, translocations, inversions, and deletions are observed in genetically unstable cells and can lead to intrachromosomal and extrachromosomal gene amplification or to a breakage-fusion bridge cycle. An inverted repeat (IR) or palindromic sequence that has the ability to form a hairpin or cruciform is often found at the breakpoint of chromosomal rearrangements (Meuth, 1989; Stark et al., 1989). These sequences are thought to cause genomic instability and are thus considered to be at-risk motifs (ARMs; Gordenin and Resnick, 1998).

Several models have been proposed to explain instability caused by IRs and palindromes (Erlich, 1989; Leach, 1994). In these models, the initial step involves an intrastrand complimentary interaction between IRs leading to extrusion of a hairpin or a cruciform secondary structure. The hairpin or cruciform structures can block progression of the replication fork and promote intra- or intermolecular template switching of the replication complex (Lobachev et al., 1998, and references therein). Alternatively, the secondary structures may be removed from the stalled replication fork by a conformation-specific nuclease, as proposed for SbcCD complex in *Escherichia coli* (Leach, 1994). Nucleolytic cleavage pro-

duces a double-strand break (DSB) that can lead to recombinational rearrangements. It has also been proposed that IR-associated DSBs might be generated through a replication-independent process (DasGupta et al., 1987). An extruded cruciform structure resembles the Holliday junction that forms during homologous recombination and potentially can be a target for resolvase or other four-way junction-cutting enzymes. Experimental evidence obtained in bacteria and eukaryotes support all three mechanisms of IR instability (Akgun et al., 1997; Erlich, 1989; Gordenin et al., 1993; Leach, 1994; Malagon and Aguilera, 1998).

The genetic control and molecular mechanism of IR-induced genomic instability has been studied extensively in *E. coli* (Erlich, 1989; Leach, 1994). While long palindromes cannot be propagated in wild-type *E. coli* cells, they are more tolerated in *sbcC* and *sbcD* mutants, although still unstable (Chalker et al., 1988; Gibson et al., 1992). The SbcCD complex has double-strand exonuclease and single-strand endonuclease activities that can cleave the hairpin loops in vitro (Connelly et al., 1999). These and other observations linking palindrome instability to replication led to the proposal that the SbcCD complex cleaves secondary structures formed by IRs during lagging-strand DNA synthesis, creating a DSB. The break can be repaired by homologous recombination, thereby reestablishing the replication fork (Leach et al., 1997).

Mre11 and Rad50 are eukaryotic homologs of bacterial SbcD and SbcC, respectively (Sharples and Leach, 1995). In yeast and humans, Mre11, Rad50, and Xrs2/Nbs1 form a tight complex that plays multiple roles in chromosome metabolism and DNA repair (reviewed in Haber, 1998). The Mre11/Rad50/Xrs2 (NBS1) complex has been implicated in telomere maintenance (Tsukamoto et al., 2001, and references therein), regulation and progression of DNA replication (Maser et al., 2001), checkpoint and damage response (D'Amours and Jackson, 2001; Grenon et al., 2001; Usui et al., 2001), nonhomologous end-joining (reviewed in Lewis and Resnick, 2000), and processing of DSBs during mitotic homologous recombination, as well as formation and end-resection of meiotic DSBs (reviewed in Pacques and Haber, 1999). Some processes involving Mre11/Rad50/Xrs2 also require Sae2/Com1. These include a checkpoint response (Usui et al., 2001), a unique type of mitotic recombination (Rattray et al., 2001), and processing of meiotic DSBs (McKee and Kleckner, 1997; Prinz et al., 1997). Based on sequence homology between Mre11 and SbcD and also between Rad50 and SbcC, it was proposed that the Mre11 complex in eukaryotes might be functionally analogous to SbcCD in bacteria, playing a comparable role in controlling IR stability (Sharples and Leach, 1995). In support of this view yeast Mre11/Rad50 and human Mre11/Rad50/Nbs1 possess endo- and exonuclease activities that can cleave and process hairpin substrates in vitro (Paull and Gellert, 1999; Trujillo and Sung, 2001).

Previously, we showed that a quasipalindrome comprised of two closely spaced inverted *Alu* sequences

¹ Correspondence: resnick@niehs.nih.gov

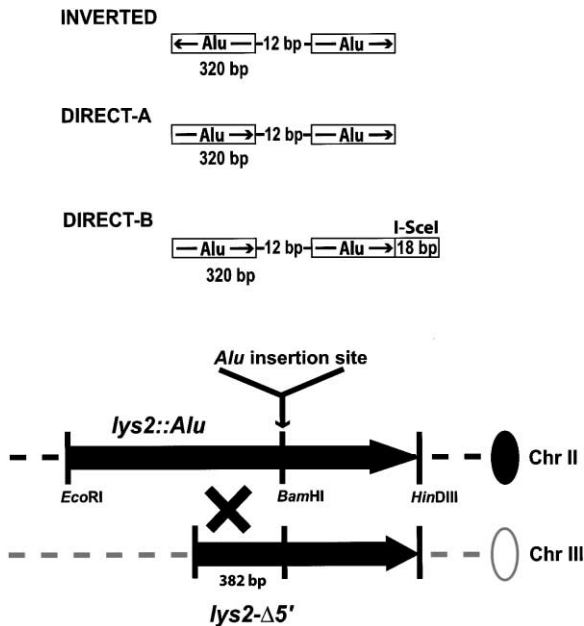


Figure 1. Recombination System to Study Instability of *Alu* Repeats in Yeast

Inverted and direct *Alu* repeats (open boxes with arrows inside) were inserted into a *Bam*HI site of the *LYS2* gene (black arrows). The position of the I-SceI site (open box) relative to insertion of the direct *Alu*s is shown. The distance between the *Alu* insertion site and the beginning of the homology region in the *lys2-Δ5'* allele is indicated (382 bp). The X denotes a recombination event generating a wild-type *LYS2* allele. The strains with insertion of an I-SceI site next to direct *Alu* repeats contained the *GAL1::I-SceI* cassette integrated into chromosome VIII (see Experimental Procedures). The centromeres of Chromosomes II and III are indicated by ovals.

(*Alu*-IR) is highly unstable in yeast *Saccharomyces cerevisiae*. The *Alu*-IR caused a 1000-fold increase in homologous recombination (Lobachev et al., 2000). In the present study, we investigate the molecular basis of *Alu*-IR-induced recombination in yeast, and we explore the role of the Mre11 complex in maintaining the stability of *Alu*-IRs. We show that an *Alu*-IR can result in a novel type of DSB in mitotic cells. Using a newly developed approach for analyzing rare mitotic chromosomal breaks, we demonstrate that resolution of a secondary structure formed by IRs results in broken molecules that are capped by a hairpin. Unlike the case for other types of DSB-induced mitotic recombination, IR-stimulated recombination strongly depends on the endonuclease activity of Mre11/Rad50/Xrs2. Failure of the *mre11*, *rad50*, *xrs2*, and *sae2* mutants to open and process the hairpins leads to chromosome inverted duplications, suggesting an additional role for the Mre11/Rad50/Xrs2 complex and Sae2 in maintaining genome stability.

Results

Experimental System

Mitotic ectopic recombination between two *lys2* alleles was used to determine the ability of an *Alu*-IR to cause genetic instability (Lobachev et al., 2000; Figure 1). An *Alu*-IR formed between identical 320 bp inverted *Alu*s

separated by a 12 bp spacer was inserted into the *LYS2* gene on chromosome II. As a control, two copies of *Alu* in direct orientation, which cannot form a hairpin or cruciform, were inserted at the same chromosomal location. Recombination between *lys2::Alu* and the *lys2-Δ5'* allele located at the *LEU2* locus of chromosome III can generate *Lys*⁺ prototrophs through simple gene conversion of the insert-containing allele or gene conversion associated with crossing-over.

MRE11, *RAD50*, *XRS2*, and *SAE2* Strongly Affect Recombination Induced by Inverted *Alu*s

An *Alu*-IR increases recombination nearly 1000-fold in a wild-type strain (Table 1; Lobachev et al., 2000). Unlike other types of recombination induced in mitotic cells, there was a strong dependence on the *MRE11*, *RAD50*, *XRS2*, and *SAE2* gene products: deletions of these genes eliminated 99% of the *Alu*-IR-stimulated recombination. The efficiency of *Alu*-IR-stimulated recombination was also reduced in *mre11-H125N* and *mre11-D56N* mutants, which lack Mre11 endonuclease activity (Moreau et al., 1999), and in a "separation-of-function" *rad50S* meiotic mutant that affects resection but not formation of meiotic DSBs (Alani et al., 1990). The effects of *mre11-H125N*, *mre11-D56N*, and *rad50S* mutations were as strong as *mre11* and *rad50* null alleles. In contrast, a low level of ectopic recombination was observed in a control strain carrying a direct *Alu* repeat, and this recombination was independent of *MRE11*, *RAD50*, *XRS2*, and *SAE2*. This result suggests that the Mre11 complex and Sae2 are specifically required for IR-induced but not for spontaneous ectopic recombination.

An *Alu*-IR Causes Chromosome II Breakage and Rearrangement

The Mre11 complex and Sae2 protein are considered to be required to remove Spo11 protein from the ends of DSBs that appear during meiosis (reviewed in Haber, 1998). The *rad50S* and Δ *sae2* mutants are unable to process protein-capped ends, and as a result, they accumulate DSBs (Cao et al., 1990; Keeney and Kleckner, 1995; McKee and Kleckner, 1997; Prinz et al., 1997). The nuclease-deficient *mre11-H125N* mutant also accumulates meiotic DSBs, indicating that it has a similar defect (Moreau et al., 1999). This suggests two possible roles for the Mre11 endonuclease during *Alu*-IR-induced mitotic recombination. An IR could form a hairpin or cruciform that is cleaved by the Mre11/Rad50/Xrs2 nuclease, generating a DSB that would strongly induce homologous recombination. In *mre11*, *rad50*, *xrs2*, and *sae2* strains that are deficient in Mre11 endonuclease, the secondary structure would be more stable, and IR-induced recombination would be greatly reduced. Alternatively, IR-mediated secondary structure could be resolved by proteins other than the Mre11 complex. In this case, a DSB would be generated with modified ends that specifically require the endonuclease activity of Mre11/Rad50/Xrs2 and Sae2 function for processing. This mechanism might be similar to the processing of meiosis-specific breaks that involve Spo11. The first hypothesis predicts that DSBs can be detected in a wild-type strain carrying an *Alu*-IR, while DSB formation should be significantly reduced in *mre11*, *rad50*, *xrs2*,

Table 1. *mre11*, *rad50*, *xrs2*, and *sae2* Mutants Strongly Affect Recombination Stimulated by Inverted *Alu* but Not Recombination Induced by I-SceI Endonuclease

Strains	Recombination Rate ($\times 10^7$)		
	Inverted <i>Alu</i>	Direct <i>Alu</i>	Direct <i>Alu</i> + I-Sce I ^a
Wild-type	1,794 (1,294–2,765) ^b	2.1 (1.7–3.5)	6,184 (4,238–7,350)
$\Delta mre11$	23 (18–35)	1.9 (1.0–2.2)	2,043 (1,522–2,645)
<i>mre11-H125N</i>	25 (16–33)	1.5 (1.2–2.8)	5,132 (3,951–8,018)
<i>mre11-D56N</i>	17 (13–36)	2.0 (1.5–3.0)	6,750 (3,977–13,240)
$\Delta rad50$	21 (14–32)	0.9 (0.5–1.5)	2,223 (1,816–3,395)
<i>rad50-S</i>	12 (6–20)	1.4 (1.0–1.5)	5,342 (4,206–12,750)
$\Delta xrs2$	19 (9–33)	3.5 (2.2–5.3)	1,862 (1,632–4,851)
$\Delta sae2$	28 (20–53)	1.3 (0.5–2.0)	6,089 (4,735–8,339)

^a Recombination rate in strains containing an insertion of direct *Alu* repeats next to the recognition site for the I-SceI endonuclease (Figure 1). In these strains a DSB was created next to the *Alu* repeats by cleavage of the I-SceI site following induction of a *GAL1::I-SceI* endonuclease gene with raffinose (see Experimental Procedures).

^b Numbers in parentheses correspond to the 95% confidence interval.

and *sae2* mutants. In the second hypothesis, *Alu*-IR-induced DSBs would be produced at the same rate in wild-type or mutants deficient in Mre11/Rad50/Xrs2 or Sae2 activities.

To address these possibilities, DNA from strains carrying an *Alu*-IR or a direct repeat was analyzed using transverse alternating field electrophoresis (TAFE) and Southern blot hybridization. Chromosome breaks were detected using a probe for *TYR1* approximately 100 kb from the insert-containing *LYS2* gene on chromosome II (Figure 2). If an *Alu*-IR causes a DSB at its insertion site on chromosome II, the TAFE gel should have one 813 kb band (intact chromosome II) and one 343 kb band. Since large DNA molecules are probed in this assay, the effect of the DSB processing (such as single-strand degradation) on the detection of the broken chromosome should be minimal.

No DSBs were detected in the control strains carrying a direct *Alu* repeat (Figure 2). In contrast, a chromosome fragment was identified at a position corresponding to the anticipated DSB in strains carrying an *Alu*-IR. The DSB frequency was ~2% of the intact chromosome II DNA for both the wild-type and $\Delta mre11$ strains. This result suggests that the Mre11 complex is involved in processing of the IR-induced DSBs, not in producing the DSB.

Surprisingly, a ~700 kb DNA fragment (nearly twice the size of the broken chromosome II product) was also present in the strain carrying the *Alu*-IR (Figure 2). This fragment was readily visible in the $\Delta mre11$ mutant (~10% of the total DNA) but was barely detectable in wild-type cells. As discussed below, this fragment is likely a chromosomal rearrangement involving an unprocessed DSB.

A DSB Occurs at the *Alu*-IR Insertion Site

In order to understand the nature of the IR-induced chromosome breaks, we developed an alternative approach for the detection and characterization of rare mitotic DSBs (Figure 3). Traditional methods for mapping of DSBs involve cutting the extracted genomic DNA with a frequent-cutting restriction enzyme that has recognition sites in the vicinity of the anticipated break. Following Southern blot hybridization, parental and broken molecules can be detected. This technique has been

applied to the analysis of meiotic recombination hotspots where the frequency of broken molecules can be as high as 30% (reviewed in Paques and Haber, 1999). Although inverted *Alu*-IRs strongly stimulate mitotic recombination, the frequency of broken chromosomes is only ~2% (see data above). Use of the previous DSB

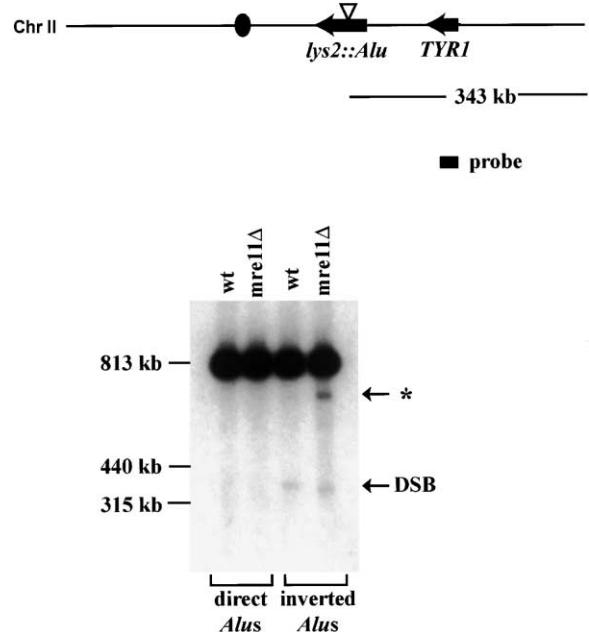


Figure 2. Breakage and Rearrangement of Chromosome II in Strains Containing Inverted *Alu* Repeats

Relative positions of centromere (black circle), *lys2::Alu* (black arrow with open triangle), and *TYR1* genes (black arrow) on chromosome II (813 kb) are shown. The distance from the *Alu* insertion site to the end of chromosome II is indicated (343 kb). Chromosomes isolated from wild-type and *mre11*Δ strains containing direct or inverted *Alu* repeats were separated by transverse alternating field electrophoresis, transferred to a nylon membrane, and hybridized with a *TYR1*-specific probe. The DSB and the asterisk next to the gel panel correspond to a breakage fragment and a chromosome rearrangement, respectively. Size markers reflect the positions of chromosome II (813 kb), chromosome IX (440 kb), and chromosome III (315 kb) on the gel stained with ethidium bromide prior to Southern blot hybridization.

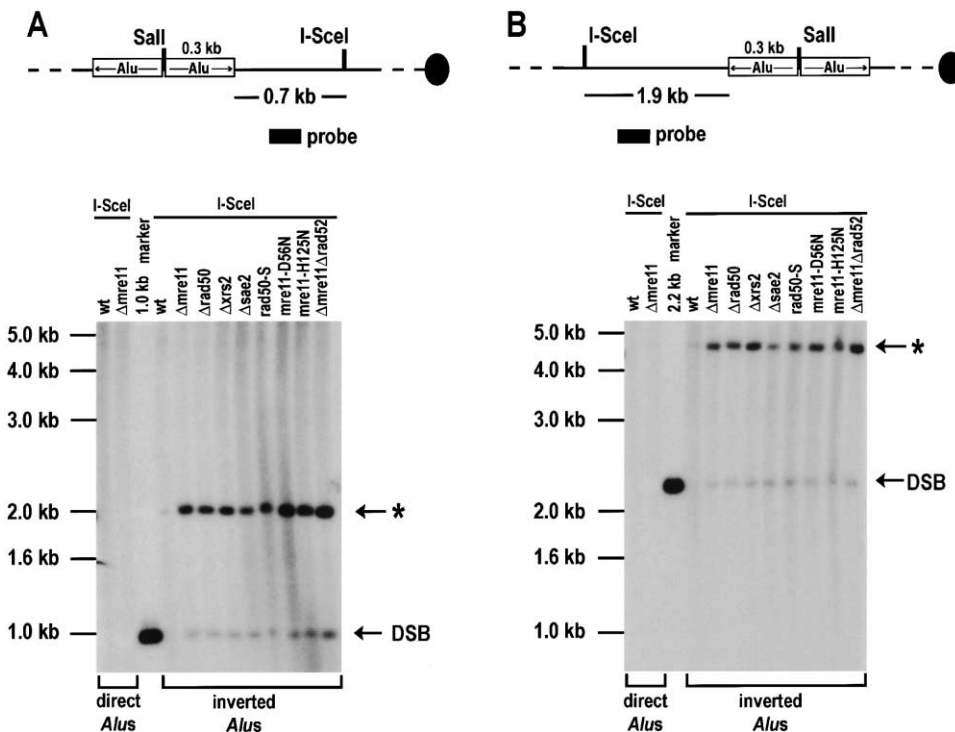


Figure 3. Analysis of DSB Formation and Rearrangements Induced by Inverted *Alu* Using the I-SceI Mapping Approach

An I-SceI site was introduced 0.7 kb (A) or 1.9 kb (B) from the insertion site of direct and inverted *Alu* repeats (open boxes with arrows inside). The chromosomal DNA from strains containing direct and inverted *Alu* repeats was embedded in agarose plugs, digested with I-SceI, and electrophoresed into the agarose gel to release the broken fragments. Southern blot hybridization was performed using *LYS2*-specific probes (solid rectangle). The DSB and the asterisk next to the gel panels correspond to broken and rearranged molecules, respectively. Horizontal arrows indicate position and the sizes of the bands corresponding to the DSB and rearranged fragments (asterisk). The 1 kb (A) and 2.2 kb (B) size markers were obtained by *SalI*-I-SceI digestion of the genomic DNA prepared from the wild-type strain containing inverted *Alu*. Also included are the positions of the 1 kb ladder markers, which were detected on the ethidium bromide-stained gel. The ability of the *Alu*-IRs to induce DSBs was assessed in the following strains: wild-type, $\Delta mre11$, $\Delta rad50$, $\Delta xrs2$, $\Delta sae2$, *mre11-H125N*, *mre11-D56N*, *rad50S*, and $\Delta mre11\Delta rad52$. Wild-type and $\Delta mre11$ strains with direct *Alu* repeats were used as controls.

mapping method yielded nonspecific bands of comparable intensity to the expected DSB bands (data not shown).

We found that the ability to map rare DSBs in mitotic cells was greatly improved if a unique restriction site (i.e., one not present elsewhere in the genome) was positioned next to the place of the anticipated break and the DNA was cut following gentle preparation of chromosomal DNA. An I-SceI recognition site was created in the *LYS2* gene either 0.7 kb upstream or 1.9 kb downstream from the *Alu*-IR (Figures 3A and 3B). Cells were lysed in agarose plugs, and chromosomal DNA was first digested with I-SceI and then separated using agarose gel electrophoresis. Digestion of the chromosomal DNA with I-SceI releases fragments that migrate into the gel only if they contain a DSB near the rare cut site. Southern blot hybridization was carried out using a *LYS2* probe adjacent to the *Alu*-IR.

No DSBs were detected in the wild-type or $\Delta mre11$ strains containing direct *Alu* repeats, nor were they observed in wild-type strains with IRs. However, when chromosomal DNA from *mre11*, *rad50*, *xrs2*, and *sae2* mutants was digested at the centromere-proximal I-SceI site, a 1.0 kb band was detected, consistent with a DSB in the *Alu*-IR region. In addition, a 2.0 kb band was also

observed (Figure 3A). A similar result was obtained when the DNA was examined from cells containing an I-SceI site centromere-distal to the IR. There was a 2.2 kb fragment that corresponded to a break in the IR region, plus there was a fragment that was twice as large (Figure 3B). Identical results were obtained using a probe specific for *Alu* sequence (data not shown).

The unprocessed DSB and double-sized rearranged molecules in *mre11* mutants could be seen at the chromosomal level as well as at the fine-scale level using the I-SceI mapping approach (Figures 2 and 3). However, DSBs could not be detected in a wild-type strain when genomic DNA was cleaved with I-SceI located close to the anticipated position of a DSB, while analysis of the chromosomal breakage showed equal amounts of the DSBs in wild-type and *mre11* mutant. This discrepancy might be due to DSBs being processed quickly by the Mre11 complex. If so, they would not be detectable by the I-SceI mapping approach where small molecules (1.0 and 2.2 kb) in the immediate vicinity of the break are probed. In the chromosomal breakage assay, much larger molecules (~343 kb) are analyzed using a probe nearly 100 kb from the *Alu*-IR so that variation in their length due to processing would not affect detection. Overall, the chromosomal and fine structure analy-

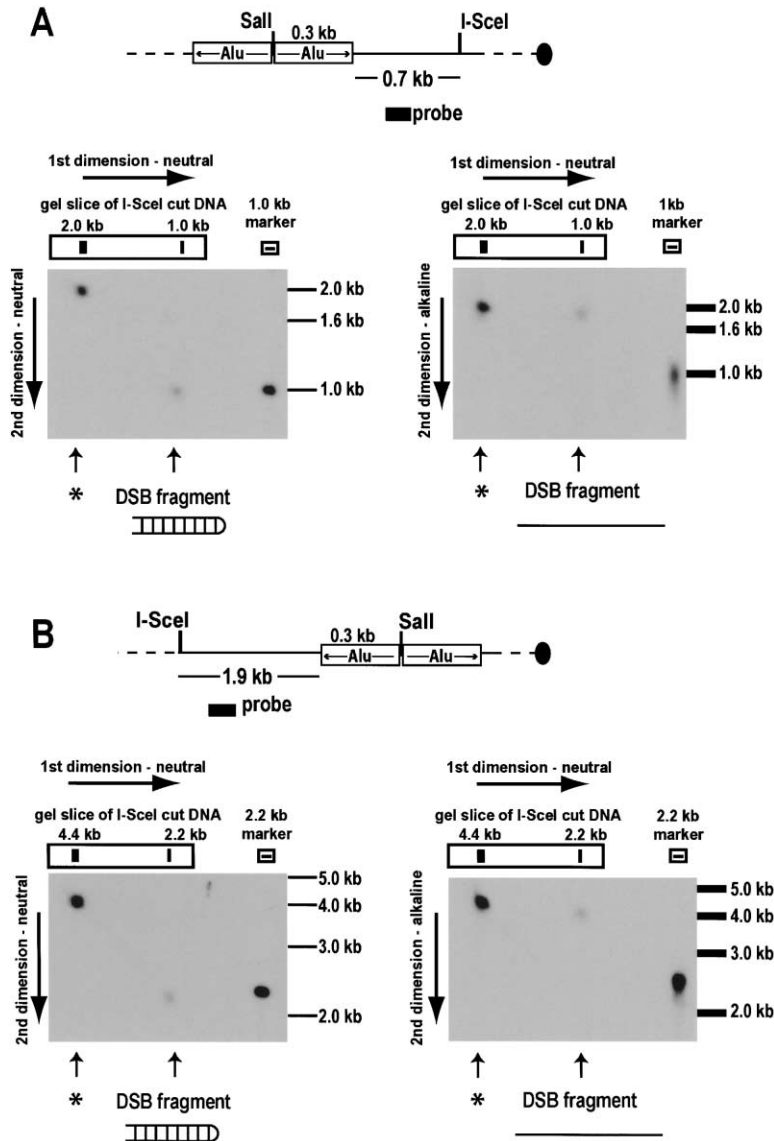


Figure 4. Analysis of the Molecular Structure of DSB Fragments by 2D Gel Electrophoresis. DSB fragments obtained by cutting at proximal (A) and distal (B) I-SceI sites were analyzed. The chromosomal DNA from a $\Delta mre11$ strain containing *Alu*-IRs was embedded in agarose plugs, digested with I-SceI, run in the first dimension on a neutral gel. Slices were cut from the gel lanes so as to include both the DSB fragments and the double-sized rearranged molecules (as shown in Figure 3, this corresponds to a region approximately 1 cm above and below the migration positions of these fragments). These slices were run in the second dimension of electrophoresis under neutral (left) or alkaline denaturing (right) conditions. Next to the slices, 1 kb (A) and 2.2 kb (B) size markers were added to a separate well, as indicated. These were obtained by *SalI*-I-SceI digestion of the genomic DNA prepared from the wild-type strain containing inverted *Alus* and serve as identical sequence controls for the fragments examined. Also indicated are the positions of standard 1 kb ladder markers that were detected on the ethidium bromide-stained gel. The DSB and rearranged fragments were identified by Southern hybridization using *LYS2*-specific probes (solid rectangle).

ses are consistent with Mre11 complex having a role in the processing but not in the initiation of the *Alu*-IR-induced DSBs.

Unprocessed DSBs Are Terminated by a Hairpin and Can Lead to an Inverted Duplication

The 1.0 and 2.2 kb DSB fragments detected in I-SceI-cleaved DNA are expected if a breakpoint occurs in the spacer region of the *Alu*-IR (*SalI* site in Figures 3A and 3B). If the *Alu*-IR induces a DSB because it forms a secondary structure, the simplest interpretation of these data is that the cruciform is recognized and cleaved by an endonuclease other than the Mre11 complex. A DSB can form if both hairpins of the cruciform are nicked in the loop. Alternatively, the cruciform can be resolved by symmetrical cuts at the base of the hairpin. In both cases, the DSB fragments will have the same size and mobility in an agarose gel, but the structure of the ends will be different. In the former case (nicking in the loop of each hairpin), the DSB fragments end in a simple

break lacking secondary structure; in the latter case (cruciform resolution), the DSB fragments end in either a nicked or an uninterrupted hairpin (if nicks are ligated). To distinguish between these two possibilities, DSB fragments were analyzed by 2D gel electrophoresis under native and denaturing (alkaline) conditions.

Chromosomal DNA was prepared from the $\Delta mre11$ strain and digested with I-SceI as described above. Electrophoresis in the first dimension was under neutral conditions. Slices were cut from the gel lanes so as to include both the DSB fragments and the double-sized rearranged molecules. These slices were run in the second dimension of electrophoresis under neutral or alkaline denaturing conditions (Figures 4A and 4B). In the case of digestion with the proximal I-SceI site followed by neutral/neutral gel electrophoresis, the expected 1.0 kb DSB and 2.0 kb rearranged fragments were detected (Figure 4A). When the second dimension electrophoresis was carried out under alkaline conditions, the 1.0 kb duplex fragment gave rise to a band that migrated as

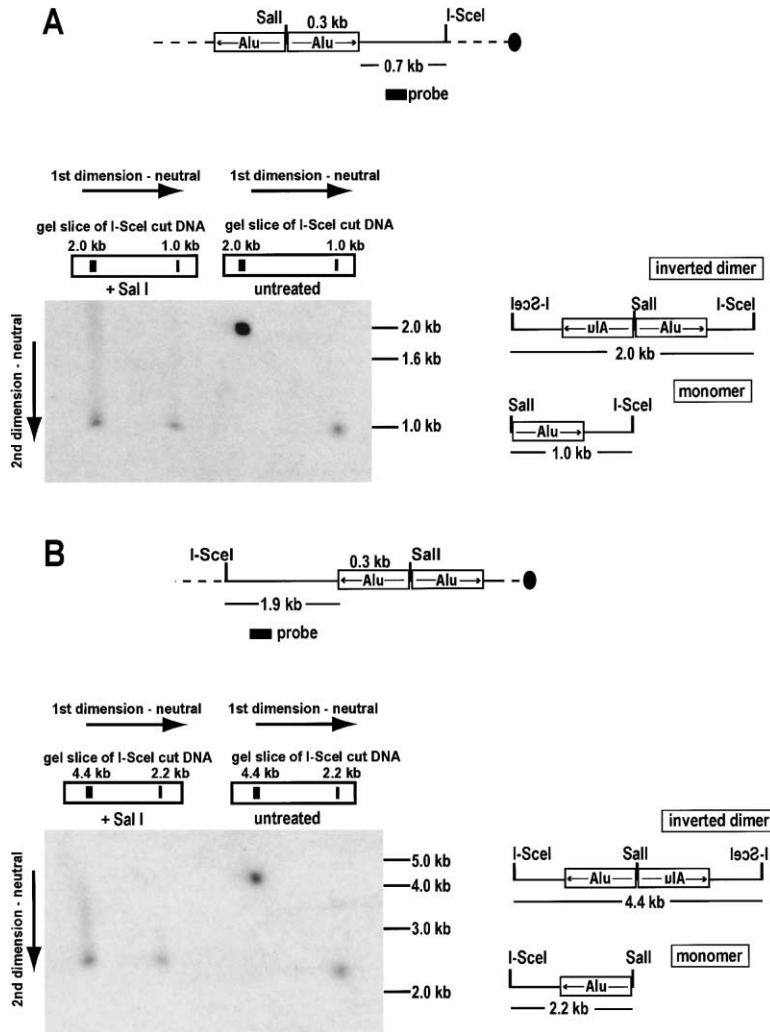


Figure 5. Identification of Inverted Dimers Induced by Inverted *Alu* Repeats Using 2D Gel Electrophoresis

Molecules obtained by cutting at proximal (A) and distal (B) I-SceI sites were analyzed. The chromosomal DNA from the $\Delta mre11$ strains containing *Alu*-IRs was embedded in agarose plugs, digested with I-SceI, and run in first dimension. Slices were cut from the gel lanes so as to include both the DSB fragments and the double-sized rearranged molecules (as shown in Figure 3, this corresponds to a region approximately 1 cm above and below the migration positions of these fragments). The slices were either treated or not with *SalI*, which is able to cut between the *Alu* repeats. They were then positioned at the top of a second neutral gel and subjected to electrophoresis. The restriction maps and sizes of the I-SceI inverted dimers and *SalI*-I-SceI monomers are diagrammed at the right of the gel panels. Also indicated are the positions of standard 1 kb ladder markers that were detected on the ethidium bromide-stained gel. The solid rectangle in the diagram at the top of (A) and (B) identifies the *LYS2*-specific probe used in Southern blot hybridizations.

2.0 kb single-strand DNA. The rearranged 2 kb duplex fragment gave rise to the expected 2.0 kb single-strand band on the alkaline gel. Similar results were observed with a distal I-SceI site (Figure 4B). The 2.2 kb DSB fragment migrated as a 4.4 kb single-strand fragment under denaturing conditions. These results indicate that the unprocessed broken molecules that appear in *mre11*, *rad50*, *xrs2*, and *sae2* mutants are terminated (i.e., capped) by a hairpin that does not have nicks in the stem. This result strongly supports the hypothesis that *Alu*-IR-induced DSBs are produced during enzymatic resolution of an extruded cruciform at the *Alu*-IR (for example see Figure 6, path I in the Discussion).

The above results provide an explanation for the larger of the two fragments detected in these experiments. The larger fragment, which is prominent in *mre11*, *rad50*, *xrs2*, and *sae2* mutants, is formed by replication of the DSB fragment containing a hairpin-capped end (see model presented in Figure 6, path I). At the chromosomal level, this should lead to acentric and dicentric chromosome II palindrome fragments.

The rearranged fragments, which were revealed by I-SceI mapping, should have an inverted dimer structure with the inverted *Alus* at the center of the symmetry. This idea was tested by analyzing the rearranged molecules

using restriction enzyme digestion and 2D gel electrophoresis. The 2D gel analysis was performed as described above, except that the DNA in the gel was digested with *SalI* prior to the native second dimension electrophoresis. *SalI* cleaves in the spacer region of *Alu*-IR (see Figure 5). Fragments were detected by Southern blotting with a *LYS2* probe. *SalI* cleaved the 2.0 kb rearranged fragment into 1.0 kb fragments (Figure 5A) and cleaved the 4.4 kb rearranged fragment into 2.2 kb fragments (Figure 5B). The restriction analysis with other enzymes that had recognition sites in the vicinity of the *Alus* insertion confirmed that the 2.0 kb and 4.4 kb rearranged fragments are inverted duplications (data not shown).

The *Alu*-IR-Induced DSB Is Distinct from a Site-Specific DSB

The biological consequences of DSBs have been studied extensively by inducing DSBs in vivo in a variety of ways, including I-SceI cleavage (reviewed in Haber, 1995). The characteristics of an I-SceI-induced DSB were compared with characteristics of the *Alu*-IR-induced DSB and the genetic controls that influence these events. A unique I-SceI site was inserted immediately adjacent to a direct *Alu* repeat (see Figure 1, DIRECT *Alu* B). In a strain

carrying this construct, the open reading frame for I-SceI endonuclease was placed under control of the inducible *GAL1* promoter and integrated into chromosome VIII. Cells grown in the presence of raffinose induce low levels of the I-SceI enzyme, which cleaves the chromosome uniquely at the recognition site. The broken chromosome can undergo homologous recombination with the *lys2-Δ5'* allele on chromosome III (Figure 1).

As expected, the induction of I-SceI led to a large increase in recombination between *lys2* alleles, comparable to the rate observed in strains containing inverted *Alu* repeats. However, the genetic control of recombination stimulated by inverted *Alu* repeats was very different from I-SceI-induced recombination (Table 1). Contrary to results with *Alu*-IR-induced recombination, the *mre11*, *rad50*, and *xrs2* null mutations caused only a 3-fold reduction in the I-SceI-induced recombination frequencies. These results are consistent with other reports that these null alleles have only a moderate effect on DSB-induced mitotic recombination (Bressan et al., 1999; Malkova et al., 1996). In *mre11-H125N*, *mre11-D56N*, *rad50S*, and *Δsae2* mutants, I-SceI-induced recombination was comparable to wild-type. Thus, *Alu*-IR- and I-SceI-induced DSBs have different consequences and are under different genetic controls.

Discussion

This study demonstrates that *Alu*-IRs can induce mitotic DSBs with terminal hairpin structures and that the Mre11/Rad50/Xrs2 complex and Sae2 protein are required for their repair. The lack of processing of hairpins in *mre11*, *rad50*, *xrs2*, and *sae2* mutants results in chromosome inverted duplications. This leads us to propose an additional role for Mre11 complex in maintaining genome stability, namely monitoring the genome to remove hairpins and thereby preventing chromosome rearrangements.

Alu-IRs Induce DSBs and Homologous Recombination in Mitotic Cells

In yeast, two types of ARMs that can adopt noncanonical DNA structures have been shown to induce genome instability through DSB formation. In meiosis, palindromes greater than 50 bp and CAG triplet repeats, which form hairpin structures in vitro, are hotspots for recombination and cause DSBs (Jankowski et al., 2000; Nasar et al., 2000). The appearance of breaks involves genes that produce DSBs during meiosis, including Spo11 (Nasar et al., 2000). In vegetatively growing yeast, a tract of 250 CTG repeats strongly induces homologous recombination and can lead to chromosomal breakage that is detectable in a *rad50* mutant (Freudenreich et al., 1998).

As shown in the present study, *Alu*-IRs induce both DSBs (Figures 2 and 3) and homologous recombination (Table 1) in mitotic cells. The *Alu*-IR-induced DSB has a terminal hairpin, consistent with the idea that closely spaced IRs can adopt a secondary structure that is a target for a nuclease. Based on our genetic analysis, the Mre11/Rad50/Xrs2 complex was a likely candidate for the nuclease. The yeast Mre11/Rad50 proteins share homology with the SbcD/SbcC nuclease that may remove

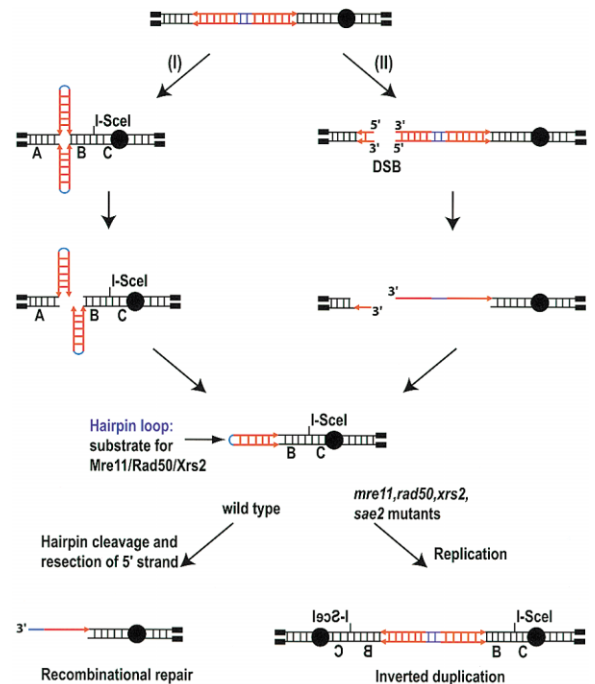


Figure 6. A Model Explaining the Generation of Chromosome Inverted Duplications by Repeats That Can Form a Fold-Back Structure in *mre11*, *rad50*, *xrs2*, and *sae2* Mutants

Presented are inverted repeats (red arrows with blue spacer region) within a chromosome. Path I: Formation of inverted duplications by unstable repeats that can extrude a cruciform from double-stranded DNA. Path II: Formation of inverted duplications following processing of DSBs in the vicinity of genetically stable (for example, distantly spaced) inverted repeats. After induction of a DSB, exonucleolytic resection exposes single-strand inverted repeat regions. Only formation of the dicentric inverted dimer is shown. A detailed description is presented in the text.

extruded palindromes in *E. coli* (Sharples and Leach, 1995). Furthermore, the Mre11 protein can nick DNA hairpins in vitro (Paull and Gellert, 1999; Trujillo and Sung, 2001). However, the frequency of *Alu*-IR-induced DSBs was similar in wild-type and *mre11* strains (~2%; Figure 2), indicating that Mre11 complex does not cleave the *Alu*-IR structure. Nevertheless, *Alu*-IR-induced recombination was 100-fold lower in *mre11*, *rad50*, and *xrs2* mutants than in the wild-type strain (Table 1). This result suggests that Mre11/Rad50/Xrs2 might participate in processing *Alu*-IR-induced DSBs. This hypothesis was confirmed using our newly developed I-SceI mapping method, which showed that *Alu*-IR-induced DSBs accumulate in *mre11*, *rad50*, and *xrs2* mutants (Figures 3A and 3B) but are not detectable in wild-type cells.

In the *mre11* mutant, the unresected DSB intermediates induced by *Alu*-IR have terminal hairpin structures (Figures 4A and 4B). This hairpin-capped DSB structure could form if an extruded cruciform is cleaved symmetrically at its base and the nicks are ligated, as described in Figure 6. The cleavage might be accomplished by a resolvase-like enzyme, a class of enzymes extensively described in prokaryotes that process Holliday junctions during recombination (reviewed in Sharples et al., 1999). A recently reported candidate resolvase in yeast is

Mms4/Eme1-Mus81 endonuclease that can cleave Holliday junctions as well as branched and replication fork substrates (Boddy et al., 2001; Kaliraman et al., 2001). However, disruption of *MUS81* or *MMS4* did not affect *Alu*-IR-induced recombination (data not shown). When *Alu*-IR-induced DSB intermediates were analyzed in a denaturing gel, covalently closed hairpins were detected but nicked hairpins were not (Figures 4A and 4B). This suggests that ligation of nicks at the cleavage site is very efficient and may be coupled to the cleavage reaction. In yeast this could be accomplished by the nonessential ligase, Lig4, and/or the essential DNA ligase, Lig1 coded by the *CDC9* gene. Deletion of the *LIG4* gene does not affect the *Alu*-IR-induced recombination (data not shown) while the effects of *cdc9* mutants remain to be determined. It is also possible that ligase activity resides in the same enzyme that carries out cleavage. For example, nicking and ligation are coupled in topoisomerase-catalyzed DNA cleavage events (Berger, 1998). Similarly, the TelN protein from *Escherichia coli* phage N15, a member of the tyrosine recombinase family, can break and rejoin cruciform DNAs to produce hairpin molecules (Deneke et al., 2000). The system we have described could be used to identify proteins that cleave and process *Alu*-IR-induced secondary structures. It would also be interesting to compare *Alu*-IR-induced changes with those due to other ARMs capable of forming secondary structures (e.g., triplet repeats).

The Endonuclease Function of the Mre11 Complex Is Required to Process *Alu*-IR-Induced DSBs

The observation that unprocessed *Alu*-IR-induced DSB intermediates accumulate in the *mre11* mutants and contain hairpins (Figures 4A and 4B) is consistent with the Mre11 complex being required for *Alu*-IR-induced recombination but not for I-SceI-stimulated recombination (Table 1). The I-SceI enzyme generates DSBs that are likely to be accessible to 5'-3' resection by several redundant exonucleases, thereby generating recombinogenic 3' protruding tails in a manner similar to that for HO-induced breaks (Paques and Haber, 1999). The Mre11 complex endo/exonuclease activity is not essential in the resection process as indicated by the relatively small reduction in I-SceI-induced recombination in the $\Delta mre11$, $\Delta rad50$, $\Delta xrs2$ mutants and the absence of any effect for *mre11-H125N*, *mre11-D56N*, *rad50S*, and $\Delta sae2$ mutations (Table 1).

The hairpin end at the *Alu*-IR-stimulated DSB might protect the broken molecule from exonucleolytic degradation. In that case, the unprocessed DSB end would not be recombinogenic, and the Mre11/Rad50/Xrs2 endonuclease would be required to open the ends to facilitate recombination events. In *mre11-H125N*, *mre11-D56N*, *rad50S*, and $\Delta sae2$ mutants, the Mre11 complex fails to open the hairpins, recombination is strongly reduced (Table 1), and unprocessed DSBs accumulate (Figures 3A and 3B).

The idea that the Mre11 complex is required to make protected DNA ends (e.g., hairpins) accessible to resection is supported by differences in processing of DSBs arising during meiotic development and enzymatically induced DSBs in mitotic cells. During meiosis, Spo11 creates DSBs in a topoisomerase II-like manner, becoming

covalently attached to the 5' ends of the broken molecule (Keeney et al., 1997). The Mre11/Rad50/Xrs2 complex along with the Sae2 protein are essential in the single-strand endonucleolytic removal of Spo11 from the DNA ends, after which the ends are 5'-resected and become recombinogenic (reviewed in Paques and Haber, 1999). In *rad50S* and $\Delta sae2$ mutants (and likely in the nuclease-deficient *mre11-H125N* and *mre11-D56N* mutants [Moreau et al., 1999]), Spo11p remains covalently linked to the 5' end and prevents DSB processing (Keeney and Kleckner, 1995). In contrast, it appears that Mre11/Rad50/Xrs2 plays a minor role in processing HO- or radiation-induced DSBs in mitotic cells. Although processing of HO-induced DSBs occurs more slowly in $\Delta mre11$, $\Delta rad50$, $\Delta xrs2$ mutants (Ivanov et al., 1994; Tsubouchi and Ogawa, 1998), recombination in $\Delta rad50$ strains is only slightly reduced (Malkova et al., 1996). Similarly, $\Delta mre11$, $\Delta rad50$, $\Delta xrs2$ mutants have only a small decrease in the frequency of radiation-induced recombination (Bressan et al., 1999). Neither *mre11-H125N*, *mre11-D56N*, nor *rad50S* mutations had any effect on HO-induced mating type switching (Moreau et al., 1999; Tsubouchi and Ogawa, 1998).

Although it is likely that *mre11-H125N*, *mre11-D56N*, *rad50S*, and $\Delta sae2$ mutants are deficient in the Mre11/Rad50/XRS2 endonuclease in vivo, these mutations could also have other effects. The *mre11-H125N* and *mre11-D56N* mutations involve amino acid changes in a conserved phosphodiesterase motif that inactivate Mre11 endonuclease activity (Moreau et al., 1999). The *rad50S* and $\Delta sae2$ mutations might directly modify the in vivo nuclease function of the Mre11/Rad50/Xrs2 complex. Alternatively, as was proposed by Usui et al. (2001), *rad50S* and $\Delta sae2$ mutations could have indirect effects by inactivating a Mre11 complex-mediated checkpoint, which, in turn, would inhibit repair by this complex. In *rad50S* and $\Delta sae2$ mutants, hairpin-capped DSBs might not be recognized as lesions, in which case they would not be processed by the Mre11/Rad50/Xrs2 complex.

Role of the Mre11/Rad50/Xrs2 Complex and Sae2p in Prevention of Inverted Chromosome Duplication and Genome Instability

We found that, in addition to inducing DSBs, the *Alu*-IRs led to the formation of rearranged molecules that were twice the size of the broken fragments (Figures 2 and 3). They accumulated in *mre11*, *rad50*, *xrs2*, and *sae2* mutants. The rearrangements were chromosomal dicentric and acentric inverted duplications with *Alu*-IRs at their centers of symmetry (Figure 4). Both duplications were detected using the I-SceI fine-scale mapping approach. However, the dicentric was not detectable at the chromosomal level. This is because its size (940 kb) and the relatively small amount would result in masking by the unbroken 813 kb chromosome (data not shown). Furthermore, the breakage of the dicentric chromosomes during mitosis (Kramer et al., 1994) would reduce their contribution to the anticipated 940 kb band.

One possible explanation for inverted dimers is that an *Alu*-IR-induced DSB initiates crossing-over between proximal and distal inverted repeats located on different sister chromatids in G2 cells. However, $\Delta rad52\Delta mre11$ double mutants had the same amount of rearranged

fragments as $\Delta mre11$ mutants (Figures 3A and 3B), indicating that the inverted duplications were not due to intermolecular recombination. Since DSB fragments have hairpin ends (Figure 4), the larger products can result from replication of these hairpin-capped fragments (Figure 6, path I). In the *mre11-H125N*, *mre11-D56N*, *rad50S*, and $\Delta sae2$ mutants, the inverted dimers accumulate, indicating that the Mre11 complex endonuclease plays an important role in preventing chromosome inverted duplications. It is likely that processing of the hairpin DSBs by the Mre11/Rad50/Xrs2 complex removes the precursors that give rise to the inverted dimers (Figure 6, path I).

Inverted repeats can form large inverted duplications (or large palindromes) in bacteria (Lin et al., 2001, and references therein) and in both lower (Huang and Campbell, 1995; Ouellette and Borst, 1991; Yasuda and Yao, 1991) and higher eukaryotes (Stark et al., 1989). Inverted duplications are implicated in early steps of intrachromosomal and extrachromosomal gene amplification during development (Delidakis et al., 1989; Yasuda and Yao, 1991), tumorigenesis (Brison, 1993), and in the appearance of drug-resistant cells (Windle and Wahl, 1992). Several models have been proposed to explain how inverted dimers are formed (Butler et al., 1996), including a *cruciform-dumbbell* model that is similar to the mechanism proposed in the present study for *Alu*-IR-induced genomic instability (Figure 6, path I). The *Alu*-IR can extrude into a cruciform and undergo cleavage, ligation, and replication to produce an inverted dimer.

As described in Figure 6, path II, the present model can also be extended to stable IRs, which are not able to adopt a cruciform structure (i.e., greater than 20 bp separation between repeats [Lobachev et al., 2000] or small repeat size) and induce DSBs on their own. The prerequisite for inverted duplication in this case is the production of a DSB in the vicinity of the IRs. A 5'-3' resection at the DSB would create a 3' single-stranded DNA tail that allows base pairing between the IR sequences and generation of a hairpin. Degradation of nonhomologous sequence followed by DNA synthesis to fill in the gap and ligation of the nick would result in a hairpin-capped DSB fragment that could replicate and form an inverted duplication. A related model was proposed by Butler et al. (1996) and has been supported by other studies (Lin et al., 2001; Qin and Cohen, 2000). In both models, an inverted duplication forms by replication of a molecule with a hairpin end. Our results suggest that the Mre11/Rad50/Xrs2 complex processes hairpin-capped DSBs induced by an *Alu*-IR. The direct involvement of the Mre11 complex and Sae2 protein in preventing an inverted duplication when a DSB is created next to a stable IR remains to be determined. However, palindromic rearrangements have been identified when a site-specific DSB is produced next to a closely spaced short IR or a widely separated long IR (Butler et al., 1996; Rattray et al., 2001). In the latter case, the frequency of rearrangements was greatly increased in *mre11-H125N*, *mre11-D56N*, *rad50S*, and $\Delta sae2$ mutants (Rattray et al., 2001).

There are many sequence motifs, including di- and trinucleotide repeats, that can adopt secondary structures and may cause genetic instability. It will be interesting to determine if these non-IR sequences can in-

duce inverted duplications and whether Mre11/Rad50/Xrs2 and Sae2 play a role. Since the human genome contains a large amount of repetitive DNA, including *Alu* sequences that can form secondary structures (Catasti et al., 1999; Lobachev et al., 2000; Stenger et al., 2001), the Mre11 complex might be crucial in preserving genome integrity, especially if there are genetic backgrounds prone to destabilization of inverted repeats (as found for yeast [Lobachev et al., 2000] or when the genome is damaged). Our results suggest an additional role for the Mre11 complex in maintaining genome stability, namely in protecting the genome against hairpin structures.

Experimental Procedures

Strains and Plasmids

All yeast strains constructed in this study were isogenic to CGL strain (*MAT α* , *ade5-1*, *his7-2*, *leu2-3,112*, *trp1-289*, *ura3- Δ*) (Lobachev et al., 2000). Construction of the pHS-I and pHS-D integrative vectors that contain, respectively, inverted and direct *Alu* repeats in the *LYS2* gene was previously described (Lobachev et al., 2000). The I-SceI site was introduced next to the insertion site of the direct *Alu* repeats by ligating *Bam*HI-linearized pHS-D plasmid with 5'-GATCTAGGGATAACAGGGTAAT-3' and 5'-GATCATTACCCTGTATCCCTA-3' annealed oligos. The resulting pHS-DSCE plasmid and pHS-I and pHS-D vectors were linearized with *Hpa*I and used to transfer inverted and direct *Alu* repeats into the chromosomal *LYS2* gene of the CGL strain by a two-step replacement procedure. To create a *lys2* interchromosomal duplication, the strains containing inverted and direct *Alu* repeats were transformed with the p305L3 plasmid cut with *Sfo*I. The p305L3 plasmid is based on the pRS305 integrative vector that contains a *Hin*DIII-*Xho*I fragment of the *LYS2* gene (*lys2- Δ 5'*) in the polylinker site. The strains with the *lys2* interchromosomal duplication and insertion of the direct *Alu* repeats next to an I-SceI site were transformed with the *Mun*I-fragment of plasmid pA4SCE to integrate a *GAL*-I-SceI cassette into the *ARG4* locus. The pA4SCE plasmid was derived from plasmid pWY2C3 (Galli and Schiestl, 1998) containing the *GAL1::I-SceI* cassette (details are available upon request).

I-SceI sites for mapping of the mitotic DSBs were introduced next to direct and inverted *Alu* repeats with help of the recently described *delitto perfetto* approach (Storici et al., 2001). Deletions of the *MRE11*, *RAD50*, *XRS2*, *SAE2*, and *RAD52* genes were made by one-step replacement using a PCR disruption technique with a kanMX module (Wach et al., 1994) or disruption plasmids. Nucleotide sequences of the oligonucleotides used for creating I-SceI sites and various gene deletions are available upon request.

Analysis of the Chromosome II Alterations

The chromosomal DNA from strains containing direct and inverted *Alu* repeats was embedded into agarose plugs using CHEF Genomic DNA Plug Kit from Bio-Rad ($\sim 1 \times 10^8$ cells/1 ml of plug). Chromosomes were separated by transverse alternating field electrophoresis (TAFE) in a Gene Line II apparatus from Beckman using 1% agarose gel in 0.25 \times TBE buffer and 75 s pulse for 48 hr. Intact chromosome II along with DSB and rearranged fragments were detected by Southern blot hybridization. Chromosomes were transferred to a nylon membrane using pressure blotter (Stratagene) and hybridized overnight at 70°C with ³²P-labeled 1325 bp *TYR1*-specific probe. Hybridization was performed in the following buffer: 6 \times SSC, 10 \times Denhardt's reagent, 1% SDS, 1 mg per ml sonicated salmon sperm DNA, 10% dextran sulfate. Membranes were washed once for 10 min at room temperature in 2 \times SSC, 0.1% SDS and three times for 20 min at 70°C in 0.1 \times SSC, 0.1% SDS. The amounts of the unbroken chromosome II, DSB, and rearranged fragments were determined using a Molecular Dynamics PhosphorImager.

I-SceI Mapping of the DSBs and 2D Gel Analysis

The chromosomal DNA for I-SceI mapping of the DSBs and 2D gel analysis was prepared similarly to that for TAFE pulse-field analysis,

except 10 times more cells per 1 ml of agarose plugs were used. Approximately 5 µg of genomic DNA embedded in agarose was digested with I-SceI (Roche). Before loading the gel, the restriction buffer was removed and plugs were incubated for 30 min at room temperature in electrophoresis buffer (1× TBE). The chromosomal DNA was separated in 0.7% agarose gel in 1× TBE at 0.7 V/cm for 16 hr. Southern blot hybridization was performed as described above. ³²P-labeled 217 bp and 247 bp probes that are homologous, respectively, to BamHI-I-SceI and I-SceI-BamHI regions of the *LYS2* gene were used for hybridization with genomic DNA.

To determine the structure of the DSB ends, the I-SceI-digested genomic DNA was analyzed by 2D gel electrophoresis. Conditions for electrophoresis in the first dimension are described above. The first-dimension lane was cut 1 cm above and below the bands of interest. For neutral/neutral 2D electrophoresis, the DNA in the gel slice was run in a 1% agarose gel containing 1× TBE buffer at 0.7 V/cm for 16 hr. For neutral/alkaline electrophoresis, the gel slice was incubated for 1 hr at room temperature in alkaline buffer (30 mM NaOH, 1 mM EDTA), and the DNA was run in to a 1% agarose containing the alkaline buffer at 0.7 V/cm for 20 hr.

The molecular structure of putative rearranged molecules was determined using 2D gel electrophoresis coupled with restriction analysis. The I-SceI-digested chromosomal DNA was run in the first dimension. The gel lane was isolated, washed twice for 30 min at room temperature in TE buffer (10 mM Tris-Cl [pH 8.0], 0.1 mM EDTA) and then incubated for 1 hr at room temperature in 10 ml of 1× *SalI* buffer. The restriction buffer was replaced with 10 ml of fresh buffer, and the agarose slice was incubated overnight at 37°C with 2500 U of *SalI* endonuclease. After digestion, the restriction buffer was replaced with 1× TBE, and the slice was gently agitated for 1 hr at room temperature. The gel electrophoresis in the second dimension was performed in 1% agarose and 1× TBE buffer at 0.7 V/cm for 16 hr. The DNA was identified by Southern blot hybridization using *LYS2*-specific probes as described above.

Genetic Techniques

Genetic and molecular procedures were previously described (Lobachev et al., 2000). Recombination was also examined following in vivo expression of I-SceI from a *GAL1* promoter. The I-SceI gene was expressed at a low level when cells were incubated on medium containing raffinose (1% bacto-yeast extract, 2% bacto-peptone, 3% raffinose, 2% bacto-agar). Fourteen independent colonies were isolated after 4 days growth at 30°C to determine the rate of I-SceI-induced recombination.

Acknowledgments

We are grateful to N. Degtyareva, J. Snipe, and J. Westmoreland for assistance in experiments, to M. Longley and R. Kokoska for critical reading of the manuscript, Nancy Kleckner for the *rad50S*-containing plasmid, and Lorraine Symington for plasmids containing *MRE11* alleles as well as helpful discussions.

Received October 25, 2001; revised December 18, 2001.

References

- Akgun, E., Zahn, J., Baumes, S., Brown, G., Liang, F., Romanienko, P.J., Lewis, S., and Jasin, M. (1997). Palindrome resolution and recombination in the mammalian germ line. *Mol. Cell. Biol.* **17**, 5559–5570.
- Alani, E., Padmore, R., and Kleckner, N. (1990). Analysis of wild-type and *rad50* mutants of yeast suggests an intimate relationship between meiotic chromosome synapsis and recombination. *Cell* **61**, 419–436.
- Berger, J.M. (1998). Structure of DNA topoisomerases. *Biochim. Biophys. Acta* **1400**, 3–18.
- Boddy, M.N., Gaillard, P.-H.L., McDonald, W.H., Shanahan, P., Yates, J.R., 3rd, and Russell, P. (2001). Mus81-Eme1 essential components of a Holliday junction resolvase. *Cell* **107**, 537–548.
- Bressan, D.A., Baxter, B.K., and Petrini, J.H. (1999). The Mre11-Rad50-Xrs2 protein complex facilitates homologous recombination-based double-strand break repair in *Saccharomyces cerevisiae*. *Mol. Cell. Biol.* **19**, 7681–7687.
- Brison, O. (1993). Gene amplification and tumor progression. *Biochim. Biophys. Acta* **1155**, 25–41.
- Butler, D.K., Yasuda, L.E., and Yao, M.C. (1996). Induction of large DNA palindrome formation in yeast: implications for gene amplification and genome stability in eukaryotes. *Cell* **87**, 1115–1122.
- Cao, L., Alani, E., and Kleckner, N. (1990). A pathway for generation and processing of double-strand breaks during meiotic recombination in *S. cerevisiae*. *Cell* **61**, 1089–1101.
- Catasti, P., Chen, X., Mariappan, S.V., Bradbury, E.M., and Gupta, G. (1999). DNA repeats in the human genome. *Genetica* **106**, 15–36.
- Chalker, A.F., Leach, D.R., and Lloyd, R.G. (1988). *Escherichia coli* *sbcC* mutants permit stable propagation of DNA replicons containing a long palindrome. *Gene* **71**, 201–205.
- Connelly, J.C., de Leau, E.S., and Leach, D.R. (1999). DNA cleavage and degradation by the SbcCD protein complex from *Escherichia coli*. *Nucleic Acids Res.* **27**, 1039–1046.
- D'Amours, D., and Jackson, S.P. (2001). The yeast Xrs2 complex functions in S phase checkpoint regulation. *Genes Dev.* **15**, 2238–2249.
- DasGupta, U., Weston-Hafer, K., and Berg, D.E. (1987). Local DNA sequence control of deletion formation in *Escherichia coli* plasmid pBR322. *Genetics* **115**, 41–49.
- Delidakis, C., Swimmer, C., and Kafatos, F.C. (1989). Gene amplification: an example of genome rearrangement. *Curr. Opin. Cell Biol.* **1**, 488–496.
- Deneke, J., Ziegelin, G., Larz, R., and Lenka, E. (2000). The proteolomerase of temperate *Escherichia coli* phage N15 has cleaving-joint activity. *Proc. Natl. Acad. Sci. USA* **97**, 7721–7726.
- Erich, D.S. (1989). Illegitimate recombination in bacteria. In *Mobile DNA*, D.E. Berg and M.M. Howe, eds. (Washington, DC: American Society for Microbiology), pp. 799–832.
- Freudenreich, C.H., Kantrow, S.M., and Zakian, V.A. (1998). Expansion and length-dependent fragility of CTG repeats in yeast. *Science* **279**, 853–856.
- Galli, A., and Schiestl, R.H. (1998). Effects of DNA double-strand and single-strand breaks on intrachromosomal recombination events in cell-cycle-arrested yeast cells. *Genetics* **149**, 1235–1250.
- Gibson, F.P., Leach, D.R., and Lloyd, R.G. (1992). Identification of *sbcD* mutations as cosuppressors of *recBC* that allow propagation of DNA palindromes in *Escherichia coli* K-12. *J. Bacteriol.* **174**, 1222–1228.
- Gordenin, D.A., and Resnick, M.A. (1998). Yeast ARMs (DNA at-risk motifs) can reveal sources of genome instability. *Mutat. Res.* **400**, 45–58.
- Gordenin, D.A., Lobachev, K.S., Degtyareva, N.P., Malkova, A.L., Perkins, E., and Resnick, M.A. (1993). Inverted DNA repeats: a source of eukaryotic genomic instability. *Mol. Cell. Biol.* **13**, 5315–5322.
- Grenon, M., Gilbert, C., and Lowndes, N.F. (2001). Checkpoint activation in response to double-strand breaks requires the Mre11/Rad50/Xrs2 complex. *Nat. Cell Biol.* **3**, 844–847.
- Haber, J.E. (1995). In vivo biochemistry: physical monitoring of recombination induced by site-specific endonucleases. *Bioessays* **17**, 609–620.
- Haber, J.E. (1998). The many interfaces of Mre11. *Cell* **95**, 583–586.
- Huang, T., and Campbell, J.L. (1995). Amplification of a circular episome carrying an inverted repeat of the DFR1 locus and adjacent autonomously replicating sequence element of *Saccharomyces cerevisiae*. *J. Biol. Chem.* **270**, 9607–9614.
- Ivanov, E.L., Sugawara, N., White, C.I., Fabre, F., and Haber, J.E. (1994). Mutations in XRS2 and RAD50 delay but do not prevent mating-type switching in *Saccharomyces cerevisiae*. *Mol. Cell. Biol.* **14**, 3414–3425.
- Jankowski, C., Nasar, F., and Nag, D.K. (2000). Meiotic instability of CAG repeat tracts occurs by double-strand break repair in yeast. *Proc. Natl. Acad. Sci. USA* **97**, 2134–2139.
- Kaliraman, V., Mullen, J.R., Fricke, W.M., Bastin-Shanower, S.A.,

- and Brill, S.J. (2001). Functional overlap between Sgs1-Top3 and the Mms4-Mus81 endonuclease. *Genes Dev.* **15**, 2730–2740.
- Keeney, S., and Kleckner, N. (1995). Covalent protein-DNA complexes at the 5' strand termini of meiosis-specific double-strand breaks in yeast. *Proc. Natl. Acad. Sci. USA* **92**, 11274–11278.
- Keeney, S., Giroux, C.N., and Kleckner, N. (1997). Meiosis-specific DNA double-strand breaks are catalyzed by Spo11, a member of a widely conserved protein family. *Cell* **88**, 375–384.
- Kramer, K.M., Brock, J.A., Bloom, K., Moore, J.K., and Haber, J.E. (1994). Two different types of double-strand breaks in *Saccharomyces cerevisiae* are repaired by similar RAD52-independent, non-homologous recombination events. *Mol. Cell. Biol.* **14**, 1293–1301.
- Leach, D.R. (1994). Long DNA palindromes, cruciform structures, genetic instability and secondary structure repair. *Bioessays* **16**, 893–900.
- Leach, D.R., Okely, E.A., and Pinder, D.J. (1997). Repair by recombination of DNA containing a palindromic sequence. *Mol. Microbiol.* **26**, 597–606.
- Lewis, L.K., and Resnick, M.A. (2000). Tying up loose ends: nonhomologous end-joining in *Saccharomyces cerevisiae*. *Mutat. Res.* **451**, 71–89.
- Lin, C.T., Lin, W.H., Lyu, Y.L., and Whang-Peng, J. (2001). Inverted repeats as genetic elements for promoting DNA inverted duplication: implications in gene amplification. *Nucleic Acids Res.* **29**, 3529–3538.
- Lobachev, K.S., Shor, B.M., Tran, H.T., Taylor, W., Keen, J.D., Resnick, M.A., and Gordenin, D.A. (1998). Factors affecting inverted repeat stimulation of recombination and deletion in *Saccharomyces cerevisiae*. *Genetics* **148**, 1507–1524.
- Lobachev, K.S., Stenger, J.E., Kozyreva, O.G., Jurka, J., Gordenin, D.A., and Resnick, M.A. (2000). Inverted Alu repeats unstable in yeast are excluded from the human genome. *EMBO J.* **19**, 3822–3830.
- Malagon, F., and Aguilera, A. (1998). Genetic stability and DNA rearrangements associated with a 2 × 1.1-kb perfect palindrome in *Escherichia coli*. *Mol. Gen. Genet.* **259**, 639–644.
- Malkova, A., Ross, L., Dawson, D., Hoekstra, M.F., and Haber, J.E. (1996). Meiotic recombination initiated by a double-strand break in rad50 delta yeast cells otherwise unable to initiate meiotic recombination. *Genetics* **143**, 741–754.
- Maser, R.S., Mirzoeva, O.K., Wells, J., Olivares, H., Williams, B.R., Zinkel, R.A., Farnham, P.J., and Petrini, J.H. (2001). Mre11 complex and DNA replication: linkage to E2F and sites of DNA synthesis. *Mol. Cell. Biol.* **21**, 6006–6016.
- McKee, A.H., and Kleckner, N. (1997). A general method for identifying recessive diploid-specific mutations in *Saccharomyces cerevisiae*, its application to the isolation of mutants blocked at intermediate stages of meiotic prophase and characterization of a new gene SAE2. *Genetics* **146**, 797–816.
- Meuth, M. (1989). Illegitimate recombination in mammalian cells. In *Mobile DNA*, D.E. Berg and M.M. Howe, eds. (Washington, DC: American Society for Microbiology), pp. 833–860.
- Moreau, S., Ferguson, J.R., and Symington, L.S. (1999). The nuclease activity of Mre11 is required for meiosis but not for mating type switching, end joining, or telomere maintenance. *Mol. Cell. Biol.* **19**, 556–566.
- Nasar, F., Jankowski, C., and Nag, D.K. (2000). Long palindromic sequences induce double-strand breaks during meiosis in yeast. *Mol. Cell. Biol.* **20**, 3449–3458.
- Ouellette, M., and Borst, P. (1991). Drug resistance and P-glycoprotein gene amplification in the protozoan parasite *Leishmania*. *Res. Microbiol.* **142**, 737–746.
- Paques, F., and Haber, J.E. (1999). Multiple pathways of recombination induced by double-strand breaks in *Saccharomyces cerevisiae*. *Microbiol. Mol. Biol. Rev.* **63**, 349–404.
- Paull, T.T., and Gellert, M. (1999). Nbs1 potentiates ATP-driven DNA unwinding and endonuclease cleavage by the Mre11/Rad50 complex. *Genes Dev.* **13**, 1276–1288.
- Prinz, S., Amon, A., and Klein, F. (1997). Isolation of COM1, a new gene required to complete meiotic double-strand break-induced recombination in *Saccharomyces cerevisiae*. *Genetics* **146**, 781–795.
- Qin, Z., and Cohen, S.N. (2000). Long palindromes formed in *Streptomyces* by nonrecombinational intra-strand annealing. *Genes Dev.* **14**, 1789–1796.
- Rattray, A.J., McGill, C.B., Shafer, B.K., and Strathern, J.N. (2001). Fidelity of mitotic double-strand-break repair in *Saccharomyces cerevisiae*: a role for SAE2/COM1. *Genetics* **158**, 109–122.
- Schar, P. (2001). Spontaneous DNA damage, genome instability, and cancer—when DNA replication escapes control. *Cell* **104**, 329–332.
- Sharples, G.J., and Leach, D.R. (1995). Structural and functional similarities between the SbcCD proteins of *Escherichia coli* and the RAD50 and MRE11 (RAD32) recombination and repair proteins of yeast. *Mol. Microbiol.* **17**, 1215–1217.
- Sharples, G.J., Ingleston, S.M., and Lloyd, R.G. (1999). Holliday junction processing in bacteria: insights from the evolutionary conservation of RuvABC, RecG, and RusA. *J. Bacteriol.* **181**, 5543–5550.
- Stark, G.R., Debatisse, M., Giulotto, E., and Wahl, G.M. (1989). Recent progress in understanding mechanisms of mammalian DNA amplification. *Cell* **57**, 901–908.
- Stenger, J.E., Lobachev, K.S., Gordenin, D., Darden, T.A., Jurka, J., and Resnick, M.A. (2001). Biased distribution of inverted and direct Alu in the human genome: implications for insertion, exclusion, and genome stability. *Genome Res.* **11**, 12–27.
- Storici, F., Lewis, L.K., and Resnick, M.A. (2001). In vivo site-directed mutagenesis using oligonucleotides. *Nat. Biotechnol.* **19**, 773–776.
- Timme, T.L., and Moses, R.E. (1988). Diseases with DNA damage-processing defects. *Am. J. Med. Sci.* **295**, 40–48.
- Trujillo, K.M., and Sung, P. (2001). DNA structure-specific nuclease activities in the *Saccharomyces cerevisiae* Rad50* Mre11 complex. *J. Biol. Chem.* **276**, 35458–35464.
- Tsubouchi, H., and Ogawa, H. (1998). A novel mre11 mutation impairs processing of double-strand breaks of DNA during both mitosis and meiosis. *Mol. Cell. Biol.* **18**, 260–268.
- Tsukamoto, Y., Taggart, A.K., and Zakian, V.A. (2001). The role of the Mre11-Rad50-Xrs2 complex in telomerase-mediated lengthening of *Saccharomyces cerevisiae* telomeres. *Curr. Biol.* **11**, 1328–1335.
- Usui, T., Ogawa, H., and Petrini, J.H. (2001). A DNA damage response pathway controlled by Tel1 and the Mre11 complex. *Mol. Cell* **7**, 1255–1266.
- Wach, A., Brachat, A., Pohlmann, R., and Philippsen, P. (1994). New heterologous modules for classical or PCR-based gene disruptions in *Saccharomyces cerevisiae*. *Yeast* **10**, 1793–1808.
- Windle, B.E., and Wahl, G.M. (1992). Molecular dissection of mammalian gene amplification: new mechanistic insights revealed by analyses of very early events. *Mutat. Res.* **276**, 199–224.
- Yasuda, L.F., and Yao, M.C. (1991). Short inverted repeats at a free end signal large palindromic DNA formation in *Tetrahymena*. *Cell* **67**, 505–516.

Note Added in Proof

Genetic results comparable to those presented here have also been found by J.A. Farah, E. Hartsuiker, K.-I. Mizuno, K. Ohta, and G.R. Smith (personal communication) with the fission yeast *Schizosaccharomyces pombe* in which a 160 bp palindrome stimulates homologous recombination in a Rad50-dependent manner. Similarly, a rad50S mutation or a mutation altering the nuclease domain of Rad32 (corresponding to Mre11) also abolishes the palindrome-stimulated recombination.